Regular Article

PHYSICAL CHEMISTRY RESEARCH
Published by the
Iranian Chemical Society
www.physchemres.org
info@physchemres.org

***Phys. Chem. Res.**, Vol. 4, No. 2, 221-230, June 2016*
DOI: 10.22036/pcr.2016.13902

Experimental and Theoretical Study of Stable Phosphorus Ylides Derived from 5-Nitroindazole in the Presence of Different Acetyelenic Esters: Furthure Insight into the Reaction Mechanism

M. Zakarianezhad* and L. Mohammadi
Department of Chemistry, Payam Noor University, Tehran, Iran
(Received 11 December 2015, Accepted 2 March 2016)

The kinetics of the reactions between triphenylphosphine **1** and dialkyl acetylenedicarboxylates **2**, in the presence of a NH-acid such as 5-nitroindazole **3**, were studied. Corresponding kinetic parameters to all reactions were evaluated, with the second order rate constant (*k*) values calculated. Effects of solvent, temperature, and reactants (dialkyl acetylenedicarboxylates) structure and concentration were evaluated on the reaction rates. Theoretical studies were performed to evaluate potential energy surfaces for all structures participating in the reaction mechanism. For all reactions, the first step was recognized as the rate-determining step, on the basis of experimental and theoretical data. Quantum mechanical calculations were utilized to clarify how the ylides exist in solution as a mixture of two geometrical isomers (*Z*- and *E*-) -the issue of majority isomer.

Keywords: NH-acid, Kinetic investigation, Theoretical study, *Z*- and *E*-rotamers, 5-Nitroindazole

INTRODUCTION

In organic synthesis, the organophosphorus compounds are known as significant reagents and intermediates [1]. One of the important groups of this category is phosphorus ylides, which is used in plenty of organic reactions [2-11]. The most important role of these compounds is converting the carbonyl groups to carbon-carbon double bonds [12]. The most important procedure among the large number of procedures accessible for the synthesis of phosphorus ylides involves the reaction of a phosphonium salt with a base [13,14]. Recently, by using a novel approach employing vinyl phosphonium salts, a procedure has been created for the preparation of this family [15,16]. Mostly, the phosphonium salts are turned into the ylides by treatment under strong base condition, however the weaker bases can be used in the case the salt is acidic enough. Michael addition of phosphorus(III) compounds such as triphenyl-phosphine to acetylenic esters leads to reactive 1,3-dipolar intermediate betaines which are not detected even at low temperature [17]. These unstable species can be trapped by a protic reagent to produce various ylides [5,11]. These ylides generally stand as a mixture of the two geometrical isomers [18,19]. In phosphorus ylides, assignment of the stability of the two *Z*- and *E*-isomers is impractical by ^{1}H and ^{13}C NMR and IR spectroscopies, mass spectrometry and elemental analysis data. Computational methods are useful tools for detection of probable reaction routes and conformational analysis of the reaction product [20,21]. To gain a better understanding of the most important geometrical parameters and investigate how these isomers can exist in two different *E*- and *Z*-forms, quantum mechanical calculations were performed on the reaction between triphenylphosphine **1**, dialkyl acetylendi-carboxylates **2** and 5-nitroindazole **3** (as a NH- heterocyclic compound) for generation of phosphorus ylides **4a-c** involving the two geometrical isomers such as *Z*- and *E*-isomers (Fig. 1) [22].

*Corresponding author. E-mail: mzakarianejad@pnu.ac.ir

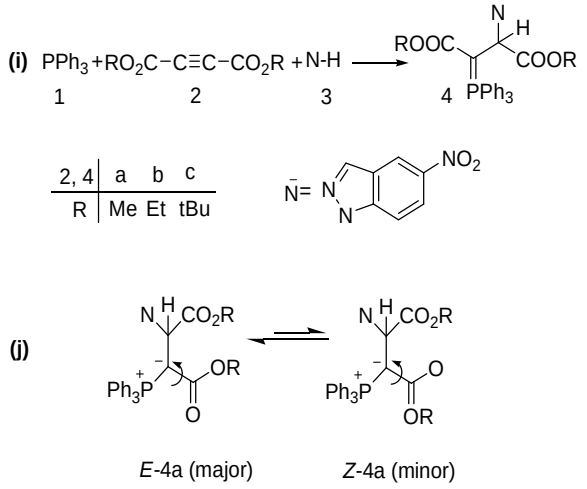

Fig. 1. (i) The reaction between triphenylphosphine **1**, dialkyl acetylenedicarboxylate **2** (**2a**, **2b or 2c**) and 5-nitroindazole **3** for generation of stable phosphorus ylides **4** (**4a, 4b or 4c**). (**j**) The two rotamers E-**4a** and Z-**4a** of ylide **4a.**

MATERIALS AND METHODS

Dialkyl acetylenedicarboxilate, triphenylphosphine and 5-nitroindazole were purchased from Fulka (Buchs, Switzerland) and used without further purification. All extra pure solvents including the dichloromethane and acetone were also obtained from Merk (Darmstadt, Germany). A Cary UV-Vis spectrophotometer model Bio-300 was employed throughout the current work. All Geometrical structures including ground and transition state were optimized at B3LYP/6-311++G(d,p) level of theory using Gaussian 09 and Gamess suite software package [23,24]. The corresponding frequencies of the structures were estimated at the same level of theory to calculate zero-point energy and check the stationary points without imaginary frequencies and the transition states with only one imaginary frequency. The solvent effect on complex stability was examined using B3LYP/6-311++G(d,p) level by applying the polarizable continuum model. Also, the intrinsic reaction coordinate (IRC) approach [25,26] was performed to ensure that the given transition state is connected to the corresponding reactants and products.

RESULTS AND DISCUSSION

Kinetic Studies

To find the appropriate wavelength, corresponding ultra-violet spectra to 3×10^{-3} M solutions of compounds **1**, **2c** and **3** were recorded over the wavelength range of 190-400 nm; the spectra are depicted in Figs. S1, S2, and S3, respectively. Then, the reaction was monitored by recording of the spectra at ambient temperature every 10 min over the whole reaction time; the result is shown in Fig. S4. Based on this result, the appropriate wavelength for thorough investigation of the reaction kinetics was found to be 355 nm. The reaction kinetics was followed by plotting UV absorbance against time at 10.0 ºC. Figure 2 shows the absorbance variations (dotted line) versus time for the 1:1:1 addition reaction among compounds **1**, **2c** and **3** at 10.0 ºC. Non-linear regression analysis can be used to automatically fit a zero, first, or second order curve to the UV absorbance values [27]. In the present research, the original experimental absorbance-versus-time data was employed to display a second-order fitted curve (solid line) with a standard deviation of 0.0022, which represented the most satisfactory fitted curve when it came to the agreement with the experimental curve (dotted line), as shown in Fig. 2.

Thus, the reaction between triphenylphosphine **1**, di-tert-butyl acetylenedicarboxylate **2c** and **3** was observed to follow the second-order kinetics. The second-order rate constant (k) was then automatically calculated at 10.0 ºC, as reported in Table 1. Continuing with the research, further kinetic studies were carried out using two concentrations of the reactants, namely 5×10^{-3} M and 7×10^{-3} M, but with the same concentration for all reactants in each run. As expected, exhibiting the same value as that of the previouse set of experiments, the second-order rate constant was observed to be independent of concentration. Therefore, the reaction was found to be of the overall order of 2.

Effects of Solvents and Temperature

To determine the effect of temperature and solvent on the rate of reaction, a number of experiments were performed with different temperatures and solvents, while keeping all other reaction parameters at the same values as those in the previous experiments. For this purpose, dichloromethane and acetone (with dielectric constants of 8.9 and 20.7,

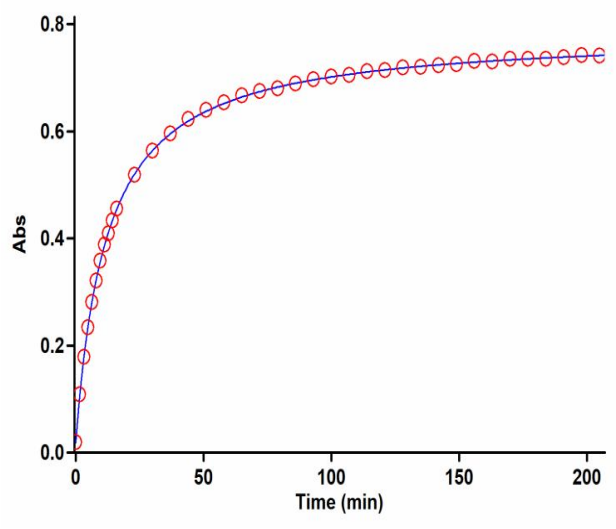

Fig. 2. Second order fit curve (solid line) accompanied by the original experimental curve (dotted line) for the reaction between compounds **1**, **2c** and **3** at 355 nm and 10.0 ºC in dichloromethane.

respectively) were chosen as suitable solvents to be evaluated. The results indicated that, for all temperatures investigated, the rate of the reaction among **1**, **2c**, and **3** was accelerated in the environment of higher dielectric constant (acetone) as compared to the one of the lower dielectric constant (dichloromethane). The fact that the second-order rate constant (lnk) of the reaction depended on reciprocal of the temperature was in line with the Arrhenius equation, giving the reaction activation energy from the slope of this plot (Table 2).

Effect of concentration

To determCine the reaction order with respect to triphenylphosphine **1** and dialkylacetylenedicarboxylate **2** (**2c**), all kinetic studies were repeated in the presence of excessive **3** (3×10^{-2} M), in which case the rate equation may be expressed as below:

$$rate = k_{obs}[1]^{\alpha}[2]^{\beta}, k_{obs} = k[3]^{\gamma} \text{ or } ln\ k_{obs} = ln\ k + \gamma\ ln[3] \quad (1)$$

Under this set of conditions, using the original experimental absorbance-versus-time data provides a second order fitted curve (solid line) to the experimental curve at 355 nm. The value of the rate constant was found to be the same as that obtained from the previous experiment. Repeating the experiments with 5×10^{-2} M and 7×10^{-2} M of **3**, the same fitted curve and rate constant were obtained. In fact, the experimental data indicated that the observed pseudo second-order rate constant (k_{obs}) was equal to the overall second-order rate constant of the reaction. It means that the value of γ is zero in Eq. (1). It seems, therefore, that the reaction is of zero order with respect to **3** (NH-acid), and second order with respect to **2**, so that the the overall order for the sum of **1** and **2** (**2c**) will be equal to 2 ($\alpha + \beta = 2$). Continuing with the research, in order to determine the reaction order with respect to triphenylphosphine **1**, the experiment was re-conducted in the presence of excessive **2** (**2c**), in which case the rate equation may be expressed as follows:

$$rate = k'_{obs}[1]^{\alpha}[3]^{\gamma} \quad k'_{obs} = k[2]^{\beta} \quad (2)$$

The original experimental absorbance-versus-time data provided a pseudo-first-order fitted curve at 355 nm, which exactly replicated the experimental curve (dotted line), as shown in Fig. 3. As a result, at $\gamma = 0$ (as determined previously), one can reasonably recognize a first order reaction with respect to compound **1** ($\alpha = 1$). Since the overall order of reaction is 2 ($\alpha + \beta + \gamma = 2$), it is obvious that $\beta = 1$, so that the reaction should be of the first order with respect to dialkylacetylenedicarboxylate **2** (**2c**). Similar observations were obtained for the reactions among (**1**, **2b** and **3**) or (**1**, **2a** and **3**). Based on the above results, a simplified reaction mechanism is proposed in Fig. 4.

Should the first step (rate constant: k_1) be the rate-determining step, the solvent may exhibit much stronger interactions with the dispersed charges in the transition state, rather than reactants of no charge. The solvent, thus, stabilizes the transition state more than it does the reactants, speeding the reaction up. Our experimental results showed that the solvent with higher dielectric constant exerts the stronger effect on the rate of reaction (see Table 1). Indeed, the results indicated the first step (k_1) of the proposed mechanism to be the rate-determining step. Thus, the rate equation can be expressed as follows:

$$rate = k_1[1][2] \quad (3)$$

Table 1. Values of Overall Second Order Rate Constant for all Reactions (**1**, **2c** and **3**), (**1**, **2b** and **3**) and (**1**, **2a** and **3**) in the Presence of Solvents such as Dichloromethane and Acetone, Respectively, at Different Temperatures

Reaction	Solvent	k_2 (cm^3 mol^{-1} S^{-1})			
		10.0 ºC	15.0 ºC	20.0 ºC	25.0 ºC
1, **2c** and **3**	Dichloromethane	3.02×10^{-30}	5.27×10^{-30}	9.10×10^{-30}	1.80×10^{-29}
	acetone	6.22×10^{-30}	8.61×10^{-30}	1.70×10^{-29}	2.61×10^{-29}
1, **2b** and **3**	Dichloromethane	6.45×10^{-29}	8.97×10^{-29}	1.18×10^{-28}	1.61×10^{-28}
	acetone	8.80×10^{-29}	1.37×10^{-28}	2.18×10^{-28}	3.02×10^{-28}
1, **2a** and **3**	Dichloromethane	6.80×10^{-29}	9.20×10^{-29}	1.30×10^{-28}	1.93×10^{-28}
	acetone	9.20×10^{-29}	2.17×10^{-28}	3.40×10^{-28}	3.90×10^{-28}

Table 2. The Activation Parameters Involving $\Delta G^{\#}$, $\Delta S^{\#}$ and $\Delta H^{\#}$ for the Reactions between (**1**, **2c** and **3**), (**1**, **2b** and **3**) and (**1**, **2a** and **3**) in Dichloromethane

Reaction	$Ea^{\#}$ (kJ mol^{-1})	$\Delta G^{\#}$ (kJ mol^{-1})	$\Delta H^{\#}$ (kJ mol^{-1})	$\Delta S^{\#}$ (kJ mol^{-1})
1, **2c** and **3**	82.77	117.64	80.35	-128.3
1, **2b** and **3**	42.32	83.49	39.94	-149.84
1, **2a** and **3**	48.73	96.46	46.32	-172.51

This equation satisfied the results obtained by UV spectrophotometry. Regarding Eq. (3) which returns the overall reaction rate, the activation parameters including $\Delta G^{\#}$, $\Delta S^{\#}$ and $\Delta H^{\#}$ are calculated for rate-determining step (the first step in this case), taken as an elementary reaction, on the basis of Eyring equation. The results are reported in Table 2.

Further Kinetic Investigations

To confirm the above observations, further experiments were performed with diethyl acetylenedicarboxylate **2b** and dimethyl acetylenedicarboxylate **2a**, under the same conditions used in the previous experiments. Reported in Table 1 are the values of the second-order rate constant (k) for the reactions among (**1**, **2b** and **3**) and (**1**, **2a** and **3**) for all solvents and temperatures investigated. The original experimental absorbance curves (dotted line) were accompanied by the second order fitted curves (solid line), which were exactly fitted with the experimental curves (dotted line), further confirming the previous observations. As seen in Table 1, the rate of the reaction increases in the environment of higher dielectric constant, and also at higher temperatures. It seems that, both inductive and steric factors for the bulky alkyl groups in **2c** tend to reduce the overall reaction rate (see Eq. (3)). In the case of dimethyl acetylenedicarboxylate **2a**, the lower the steric and

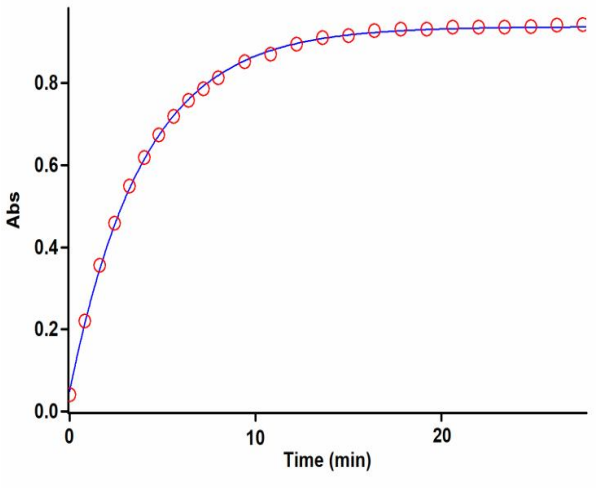

Fig. 3. Pseudo first order fit curve (solid line) for the reaction between **1** and **3** in the presence of excess **2** (**2c**) (10^{-2} M) at 355 nm and 10.0 °C in dichloromethane.

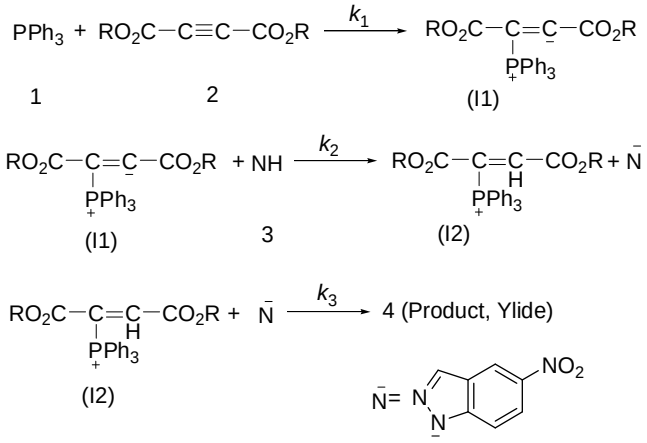

Fig. 4. Proposed mechanism for the reaction between **1**, **2** (**2a**, **2b** or **2c**) and **3** for generation of phosphorus ylides **4a-c**.

inductive effects of the dimethyl groups, the larger the effect exerted on the rate of reaction. As seen in Table 2, enthalpy of activation ($\Delta H^{\#}$) is considerably increased as the reaction goes from **4a** or **4b** to **4c**. Significant negative value of the entropy of activation ($\Delta S^{\#}$) suggests that the transition state is more ordered than the starting reactants. Moreover, the transition state is more ordered in the presence of **2a** and **2b**, rather than that in the presence of **2c**. As the entropy of activation ($\Delta S^{\#}$) further tends towards larger negative values, the enthalpy of activation ($\Delta H^{\#}$) is observed to decrease. However, more remarkable decrease (in $\Delta S^{\#}$) and increase (in $\Delta H^{\#}$) were observed as the reaction went from **4a** or **4b** to **4c.**

Theoretical Study

Energetics and geometries in gas phase. To gain further insight into the reaction mechanism, all structures were optimized at B3LYP/6-311++g(d,p) level of theory. Two different reaction paths were predicted which corresponded to the nucleophilic attack of triphenyl-phosphine **1** to dimethyl acetylenedicarboxylate **2a** in different directions. The potential energy profiles for the two pathways, **E** and **Z**, are presented in Fig. 5. The optimized geometries of all structures are demonstrated in Fig. 6. As seen, the first step is initiated with the nucleophilic attack of atom P, in the structure of triphenylphosphine **1**, to atom C6 of dimethyl acethylene-dicarboxylate **2**, so as to form **I1**, passing through **Ts1**. The second step includes the conformational evolution of **I1** into **I1'**. Then, **I'** can be formed as **I2,** *via* hydrogen bonding, to **3**. The third step is the intermolecular proton transfer from atom N60 to atom C5 in structure **Ts2**. From the results, the fourth step proposed in the experimental section is not possible to perform. The formation of the N60-C5 bond was expected to pass through a transition state; however, due to high affinity of S^- towards connecting to C5, the process was not observed. Thus, the overall reaction proceeded via two barrier heights, namely 51.84 (67.74) and 15.65 (14.08) kJ mol^{-1}, respectively, (figures in parentheses refer to the path **Z**). With 36.19 (53.66) kJ mol^{-1} more energy barrier than the third step, the first step of the reaction was recognized as the rate-determining step. Comparing potential energy surfaces, one can see that, except for **P-*E***, all structures (including intermediates and transition states) were more stable in *E*-form, rather than Z-form.

With a relative enthalpy of -103.46 (17.09 kJ mol^{-1}), the overall reaction is exothermic, while a relative free energy of -110.19 (13.34 kJ mol^{-1}) proves the reaction to be spontaneous. Even though in the actual synthesis of stable phosphorous ylide in the presence of 5-nitroindazole, **P-*E***

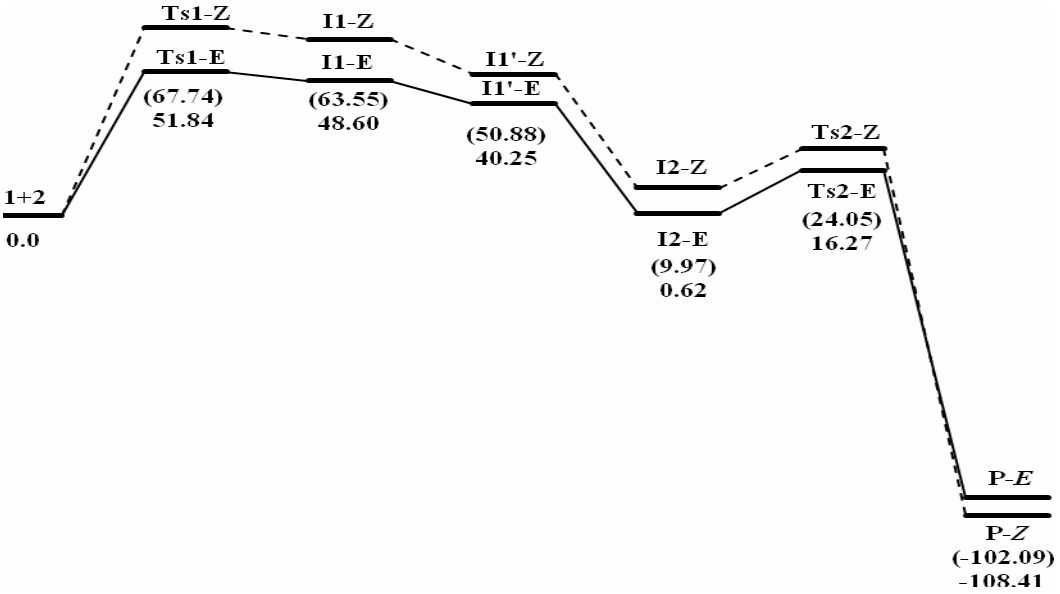

Fig. 5. Potential energy diagram (including zero point energy) along the different reaction pathways (**E** and **Z**) at the B3LYP/6-311++G(d,p) level of theory. Relative energies are in kJ mol^{-1}.

was recognized as the major isomer (57%) [22], the theoretical results had indicated **P-*E*** to be 6.32 kJ mol^{-1} less stable than **P-*Z***. The reaction mechanism was then be investigated in further detail. The associated energy barrier with the first step of the path **E** was less than the path **Z**, so that a kinetic stability of 15.90 kJ mol^{-1} was created along path **E**. It was obvious that the reaction tended to proceed along the path **E** with less energy barrier, leading to the production of a major product (**P-*E***) which is less stable than **P-*Z***. If we assume that the products **P-*E*** and **P-*Z*** can be converted into each other, then the **P-*Z***, as the thermodinamically more stable isomer, should be the major product, contrary to the experimental results. Indeed, the results indicated that the process was associated with an energy barrier of either 74.13 or 71.06 kJ mol^{-1} (depending on the orientation of COOMe group), which was relatively high and non-plausible (Fig. 7). So, from the theoretical results, the majority of product **P-*E*** was attributed to the kinetic priority of path **E**, as compared to path **Z**. Additionally, **I1-Z** and **I2-Z** can be converted into more stable structures of **I1-E** and **I2-E**, by passing through small barrier heights of 14.31 and 11.14 kJ mol^{-1}, respectively. So, changing the reaction path to the path **E**, led to the production of **P-*E*,** as the major product (Fig. 7).

Energetics and geometries in solution. To study the effect of solvent on the potential energy surfaces, condensed phase calculations in dichloromethane (ε = 9.00) were carried out with the polarizable continuum model (PCM). The potential energy profiles for two pathways **E** and **Z** are presented in Fig. S5. As indicated by the results, the energy barriers of the first and the third steps along the path **E** are decreased by the value of 16.4 and 5.76 kJ mol^{-1}, respectively, compared to those in gas phase. Along the path **Z**, the energy barriers of the first and third step of the reaction are reduced by 24.03 and 5.36 kJ mol^{-1}, respectively, compared to those in gas phase. In both paths, the energy barrier of the first step is considerably larger than that of the third step. Thus, the first step of the reaction was once more confirmed to be the rate-determining step. Because of lower energy barrier of the first step along path **E**, it was kinetically preferable over the path **Z**. The energy barrier of **P-*E*** to **P-*Z*** conversion was seen to increase to 76.24 and 73.69 kJ mol^{-1} for two paths, respectively (Fig. S6). However, the barrier height of the **I1-Z** to **I1-E** conversion increased to 16.47 kJ mol^{-1}, while that

of the **I2-Z** to **I2-E** conversion decreased to 10.11 kJ mol^{-1}, compared

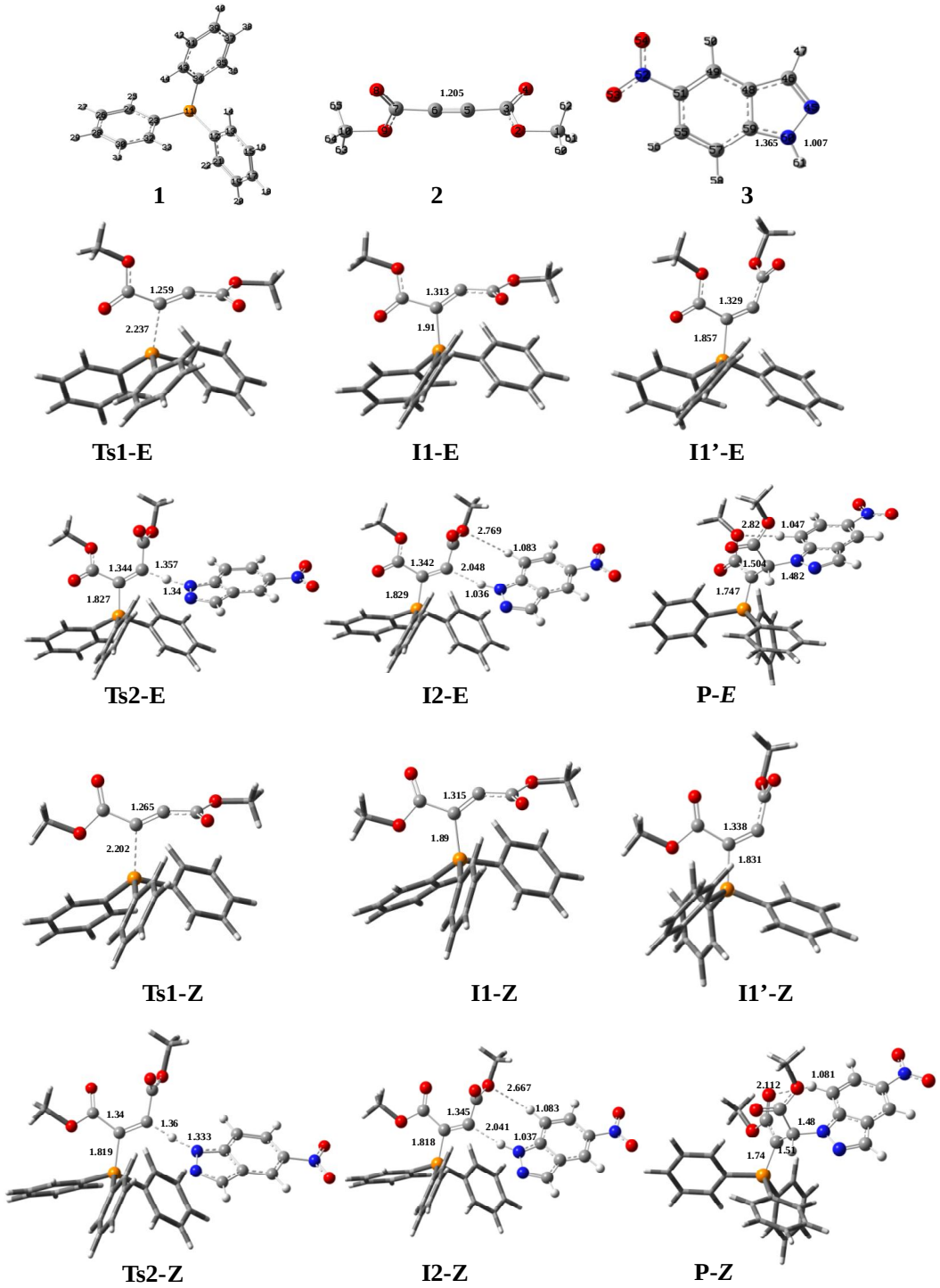

Fig. 6. Optimized geometries of all structures (including reactants, transition states, intermediates and products) along the reaction paths **E** and **Z** at the B3LYP/6-311++G(d,p) level of theory.

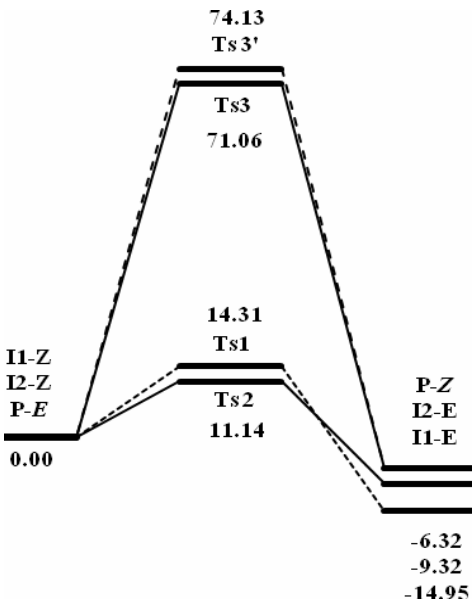

Fig. 7. Potential energy diagram (kJ mol^{-1}) (including zero point energy) for conversion pathways (P-*E*⟶P-*Z*, I1-Z⟶P-E and I2-Z⟶I2-E) at the B3LYP/6-311++G(d,p) level of theory.

to those in gas phase. Results in solvent showed that, similar to gas phase, kinetic preference of the path **E** and the high barrier height of **P-*E*** to **P-*Z*** conversion contributed to the majority of **P-*E***.

Reaction Rate

Quantum calculation results, in both gas phase and dichloromethane, illustrated that the first energy barrier was significantly higher than the second one, confirming the first step would be the rate-determining step.

Similar to overall rate constant of the reaction, the experimental rate constant of the first step was found to be 1.93×10^{-28} cm^3 mol^{-1} S^{-1} in dichloromethane at 298.15 K. Theoretical rate constant of the reaction was seen to range from 1.60×10^{-25}-9.89×10^{-30} cm^3 mol^{-1} S^{-1} in various mediums and along various reaction paths; this was well in agreement with the experimental values. From the results, the exhausted energies of the reaction in gas phase and in solution were 67.49 (81.83 kJ mol^{-1}) and 45.33 (52.44 kJ mol^{-1}), respectively, implying that the reaction path **E** was energetically more favorable , both in gas phase and in solution.

CONCLUSIONS

Investigated in this research, both experimentally and theoretically, was the reaction between triphenylphosphine **1**, and dialkylacetylenedicarboxylates **2** in the presence of a NH-acid such as 5-nitroindazole **3**. The results can be summarized as follows:

1. The overall reaction order followed second-order kinetics, with the first order dependent on the concentrations of triphenylphosphine **1** and dialkyl acetylenedicarboxylates **2**.
2. Under the same conditions, the activation energy for the reaction with di-tert-butyl acetylenedicarboxylate **2c** was higher than those with the other two compounds, namely diethyl acetylenedicarboxylate **2b** and dimethyl acetylenedicarboxylate **2a**, in all solvents investigated.
3. All reactions had the rates increased in solvents with higher dielectric constants. This could be attributed to the differences in reactant stabilization versus activated complex in the transition state stabilization, by different solvents.
4. The steric effect of bulk alkyl groups in dialkyl acetylenedicarboxylates, accompanied by the correspondingly greater inductive effect, reduced the overall reaction rate. Results indicated more important role played by the steric factor of the bulky alkyl groups in **2c**, rather than its inductive effect.
5. Referring to the experimental and theoretical data, the first step of the proposed mechanism (k_1) was recognized as the rate-determining step.
6. Theoretical results could explain the majority of **P-*E*** isomer in spite of its lower stability.
7. Even though the experimental results indicated the reaction to proceed via a three-step path, the theoretical studies proved the reaction to proceed through two steps only.

REFERENCES

[1] Alajarin, M.; Constant, S.; Lacour, J.; Marque, S.; Tordo; P.; Lopez-Leonardo, C.; Llamas, P., New acpects in Phosphorus Chemistry V, springer, New York, **2005**.

[2] Batczewski, P.; keglevich, G.; Narukula, R.; Noe, M.; Pajkert, R.; Perosa, A.; Selva, M.; Skalic, J. Organophosphorus Chemistry, Vol. 43, RSC, UK, **2014**.

[3] Murphy, P. J., Organophosphorus Reagents: A Practical Approach in Chemistry, Vol. 43, Oxford University, New Yourk, **2004**.

[4] Timparley, C. M., Synthetic Methods: Organo-phosphorus(V) Chemistry. Academic press, UK, **2014**.

[5] Kalantari, M.; Islami, M. R.; Hassani, Z. Saidi, K., Synthesis of dimethyl-1-(trifluoromethyl)-3H-pyrrolizine-2,3-dicarboxylate using phosphorus compounds. *Arkivoc* **2006**, *x*, 55-62.

[6] Islami, M. R.; Mollazehi, F.; Badiei, A.; Sheibani, H., Serendipitous synthesis of 1, 4-benzothiazin derivativ es using 2-[(2-aminophenyl)disulfanyl aniline. *Arkivoc* **2005**, *xv*, 25-29.

[7] Maghsoodlou, M. T.; Hazeri, N.; Habibi-Khorassani, S. M.; Moeeni, Z.; Marandi, G.; Lashkari, M.; Gasemzadeh, M.; Bijanzadeh, H. R., Water-acetone media enforced chemoselective synthesis of 2-substituted pyrrole stable phosphorus ylides from reaction between pyrrole and acetylenic esters in the presence of triphenylphosphine. *J. Chem. Res.*, **2007**, *10*, 566-568. DOI: 10.3184/030823407X255560.

[8] Anary-Abbasinejad, M.; Anaraki-Ardakani, H.; Hosseini-Mehdiabad, H., One-pot synthesis of stable phosphorus ylides by three-component reaction between dimethyl acetylenedicarboxylate, semicarbazones, and triphenylphosphine. *Phosphorus Sulfur*, **2008**, *183*, 1440-1446. DOI: 10.1080/ 10426500701670725.

[9] Hassanabadi, A.; Anary-Abbasinejad, M.; Dehghan, A., Three-component reaction of triphenylphosphine, dimethyl acetylenedicarboxylate, and aldehyde benzoylhydrazones: an efficient one-pot synthesis of stable phosphorus ylides. *Synthetic Commun*, **2009**, *39*, 132-138.

[10] Anaraki-Ardakani, H.; Sadeghian, S.; Rastegar, F.; Hassanabadi, A.; Anary-Abbasinejad, M., Three-component reaction of triphenylphosphine, acetylenic esters, and arylsulfonyl hydrazines: an efficient one-pot synthesis of stable-nitrogen-substituted phosphourus ylides. *Synthetic Commun*, **2008**, *38*, 1990-1999. DOI: 10.1080/00397910801997785

[11] Zakarianezhad, M.; Habibi-Khorassani, S. M.; Khajeali, Z.; Makiabadi, B.; Feyzi, M.; Taheri, A., Mechanistic investigation of the reaction between triphenylphosphine, dialkyl acetylenedicarboxylates and pyridazinone: a theoretical, NMR and kinetic study. *Reaction Kinetics, Mechanisms and Catalysis*, **2014**, *111*, 461-474. DOI: 10.1007/S11144-013-0653-3.

[12] Maryanoff, B. E.; Reit, A. B., The Wittig olefination reaction and modifications involving phosphoryl-stabilized carbanions. Stereochemistry, mechanism, and selected synthetic aspects. *Chem. Rev.*, **1989**, *89*, 863-927. DOI: 10.1021/cr00094a007

[13] Fitjer, L.; Quabeck, U., The Wittig reaction using potassium-tert-butoxide high yield methylenations of sterically hindered ketones. *Synth. Commun.*, **1985**, *15*, 855-864. DOI: 10.1080/00397918508063883

[14] Yavari, I.; Ali-Asgari, S.; Porshamsian, K.; Bagheri, M., Efficient synthesis of functionalized bis-(4-oxo-1,3-thiazolan-5-ylidene)acetates. *J. Sulfur. Chem.*, **2007**, *28*, 477-482. DOI: 10.1080/ 17415990701471364

[15] Ramazani, A.; Souldozi, A., Dipotassium-hydrogen-phosphate-powder-catalyzed stereoselective C-vinylation of diphenylacetonitril. *Phosphorus Sulfur*, **2005**, *180*, 2801-2804. DOI: 10.1080/ 10426500500272160

[16] Yavari, I.; Alizadeh, A. A., A simple approach to the synthesis of 1,4-bis (arylsulfonyl) tetrahydro-pyrazine-2,5-diones). *Monatsh Chem.*, **2003**, *134*, 435-438. DOI: 10.1007/s00706-002-0533-4.

[17] Shahraki, M.; Habibi-Khorassani, S. M., Kinetic spectrophotometric approach to the reaction mechanism of pyrrole phosphorus ylide formation based on monitoring the zwitterionic intermediate by using the stopped-flow technique. *J. Phys. Org. Chem.*, **2015**, *28*, 396-402. DOI: 10.1002/poc.3424

[18] Habibi-Khorassani, S. M.; Shahraki, M.; Maghsoodlou, M. T.; Erfani, S., Dynamic ^{1}H NMR studies of hindered internal rotations in the synthesized particular phosphorus ylide: Experimental and theoretical approaches. *Spectrochim. Scta A*, **2015**, *145*, 410-416. DOI: 10.1016/j.saa.2015.02.084.

[19] Shahraki, M.; Habibi-Khorassani, S. M.; Ebrahimi, A.; Maghsoodlou, M. T.; Ghalandarzehi, Y. Intramolecular hydrogen bonding in chemoselective synthesized 2-substituted pyrrole stable phosphorus ylide: GIAO, AIM, and NBO approaches. *Struct. Chem.*, 2012, *24*, 623-635. DOI: 10.1007/s11224-012-0114-z.

[20] Chahkandi, B.; Chahkandi, M.; Ashrafi, B. Conformational analysis of N- and C-terminally protected tripeptide model glycyl-isoleucine-glycyl: An *ab initio* and DFT study. *Phys. Chem. Res.*, **2014**, *2*, 68-75.

[21] Izadyar, M.; Kheirabadi, R. A theoretical study on the structure-radical scavenging activity of some hydroxyphenols. *Phys. Chem. Res.*, **2016**, *4*, 73-82.

[22] Maghsoodlou, M. T.; Hazeri, N.; Habibi-Khorassani, S. M. ; Kakaei, R.; Nassiri, M., A simple synthesis of stable phosphorus ylides from indole and some of its derivatives. *Phosphorus Sulfur*, **2006**, *181*, 913-919. DOI: 10.1080/10426500500272160.

[23] Frisch, M. J.; Trucks, G. W.; Schlegel, H. B.; Scuseria, G. E.; Robb, M. A.; Cheeseman, J. R., Gaussian, Inc: Wallingford (CT), **2009**.

[24] Granovsky, A. A. PC Gamess Version 7.1.G, **2009**. Available from: http://classic.chem.msu.su/gran/gamess/index.html/.

[25] Gonzalez, C.; Schlegel, H. B., Reaction path following in mass-weighted internal coordinates. *J. Phys. Chem.*, **1990**, *94*, 5523-5527. DOI: 10.1021/j100377a021.

[26] Gonzalez, C.; Schlegel, H. B., An improved algorithm for reaction path following. *J. Chem. Phys.*, **1989**, *90*, 2154-2161. DOI: 10.1063/1.456010

[27] Schwartz, L. M.; Gelb, R. I., Alternative method of analyzing first-order kinetic data. *Anal. Chem.*, **1978**, *50*, 1592-1594. DOI: 10.1080/10426500500272160

[28] Eckart, C., The penetration of a potential barrier by electrons. *Phys. Rev.*, **1930**, *35*, 1303. DOI: 10.1103/Phys.Rev.35.1303.